

EXPERIMENTAL CHARACTERIZATION AND NEURAL NETWORK PREDICTION OF DYNAMIC BEHAVIOR OF ZTA WITH SrCO₃ AND MgO

by

ALI ARAB

UNIVERSITI SAINS MALAYSIA

2016

**EXPERIMENTAL CHARACTERIZATION AND NEURAL
NETWORK PREDICTION OF DYNAMIC BEHAVIOR OF ZTA
WITH SrCO₃ AND MgO**

by

ALI ARAB

**Thesis submitted in fulfilment of the requirements
for the degree of
Doctor of Philosophy**

March 2016

ACKNOWLEDGMENTS

In the name of God the most gracious the most merciful

This dissertation would not have been possible without the guidance and help of several individuals who contributed and extended their valuable assistance in the preparation and completion of this study.

I wish to express my gratitude to my main supervisor, Assoc. Prof. Dr. Roslan bin Ahmad, for the inspiration, motivation and professionally guiding me to successfully complete my research work. I would like to also thank him for providing me with outstanding research facilities and numerous technical discussions which I found to be very valuable to my research. His constant enthusiasm and insightfulness will be a model for my career.

I would like to express my very great appreciation to Professor Hj. Zainal Arifin b. Hj. Ahmad for his contribution on the co-supervision. His encouragement, valuable suggestions, and support from the initial to the final stage of my work enabled me to understand and develop the subject.

Next, I would like to convey my special thanks to heads of School of Mechanical Engineering and School of Material and Mineral Resource Engineering and all staffs of these Schools, for their kind assistant and supports. Without their kind cooperation, this study may not be completed on time.

I would like to thank my beloved wife for her endless love and support for encouraging me in all my efforts to this day. Lastly, my special and deepest appreciation and thanks go to both my parents. Their constant support, encouragement gives warmth and strength to me. They always are there to share my success as well during sad and down time. Their inspiration, understanding, patience, and support, help me to complete this thesis and no words are adequate to express my appreciation to both of them.

TABLE OF CONTENTS

	Page
Acknowledgments.....	ii
Table of contents.....	iii
List of Tables.....	vii
List of Figures.....	viii
List of Abbreviations.....	xvi
List of Symbols.....	xvii
Abstrak.....	xviii
Abstract.....	xiv
CHAPTER 1- INTRODUCTION	
1.1 Research background	1
1.2 Problem statement	5
1.3 Objective:	7
1.4 Project approach	7
1.5 Scope and limitation	8
1.6 Structure of thesis	9
CHAPTER 2- LITERATURE REVIEW	
2.1 Introduction and chapter layout.....	11
2.2 Ceramic armor	11
2.3 Ballistic and dynamic test for ceramic armor.....	14
2.4 Split Hopkinson Pressure Bar (SHPB)	18
2.4.1 Historical Development.....	18
2.4.2 SHPB Theory.....	20

2.4.3	Split Hopkinson for brittle material.....	22
2.4.4	Confinement	26
2.5	Ceramic dynamic failure	30
2.5.1	Phenomenological damage mechanics	31
2.5.2	Micromechanical	31
2.5.3	Experimental failure of ceramic under the dynamic load	34
2.6	Zirconia Toughened Alumina	36
2.6.1	ZTA application in the ceramic armor	36
2.7	ZTA Properties	39
2.7.1	Alumina:	41
2.7.2	Zirconia:	42
2.7.3	ZTA toughening mechanisms.....	43
2.7.3.1	Micro-crack toughening.....	43
2.7.3.2	Stress induced transformation toughening:.....	43
2.7.4	ZTA additive	44
2.7.4.1	MgO	45
2.7.4.2	SrO	46
2.7.4.3	Cr ₂ O ₃	47
2.7.4.4	CeO ₂	48
2.7.4.5	CaCO ₃	49
2.8	Using Artificial Neural Network for Material Model	50
2.8.1	Artificial Neural network:	50
2.8.2	Artificial Neural Network for Material Model.....	51
2.9	Concluding remarks	53
Chapter 3- Experimental details and analysis		
3.1	Introduction	55
3.2	Sample preparation.....	56
3.2.1	Raw materials	56
3.2.2	Sample preparation.....	57
3.2.2.1	Preparing the ZTA sample (with different amount of YSZ).....	57
3.2.2.2	Preparing the ZTA-SrCO ₃ samples.....	59
3.2.2.3	Preparing the ZTA-MgO samples.....	60

3.3	Material Characterization	61
	3.3.1 Phase Analysis by X-ray Diffractometer (XRD).....	61
	3.3.2 Microstructure Observation.....	61
	3.3.3 Density and porosity.....	61
3.4	Mechanical testing.....	62
	3.4.1 Vickers Hardness and Fracture Toughness	62
	3.4.2 Split Hopkinson Pressure Bar (SHPB) modified for brittle material .	63
	3.4.2.1 Attachment of tungsten carbide platen.....	65
	3.4.2.2 Pulse shaper.....	67
	3.4.2.3 Manipulation of Stress-strain data	69
	3.4.2.4 Confinement.....	71
3.5	Machine learning	74
	3.5.1 Neural network Multilayer Perceptron (MLP).....	74
	3.5.2 Time series.....	76
	3.5.3 Supporting vector regression.....	78

Chapter 4- Result and Discussion

4.1	Introduction	81
4.2	Characterization of raw materials.....	81
	4.2.1 Al ₂ O ₃	81
	4.2.2 YSZ.....	83
	4.2.3 SrCO ₃	85
	4.2.4 MgO.....	87
4.3	Investigation on the effect of amount YSZ on the ZTA properties.....	88
	4.3.1 Materials characterization	88
	4.3.2 Dynamic properties	93
4.4	Investigation of the effect of amount SrCO ₃ on the ZTA properties	98
	4.4.1 Materials characterization	98
	4.4.2 Dynamic properties	104
4.5	Investigation of the effect of MgO amount on the ZTA properties	110
	4.5.1 Materials characterization	110
	4.5.2 Dynamic properties	116
4.6	Relationship between the dynamic strength, hardness	119

4.7	Confinement effect	121
	4.7.1 Confinement on ZTA -20 wt.% MgO Samples.....	121
4.8	Machine learning	124
	4.8.1 MLP.....	124
	4.8.2 SVR	125
	4.8.3 Time Series.....	127

Chapter 5- Conclusion and Future Recommendation

5.1	Conclusion.....	131
5.2	Future Recommendation	132
	References	134

Appendices

LIST OF TABLES

		Page
Table 2.1	Mechanical properties of ceramic and their role in armor (Karandikar & Evans, 2009)	14
Table 2.2	Literature review of dynamic tests study by SHPB	23
Table 2.3	Hardness and fracture toughness of different amount of zirconia (Oungkulsolmongkol et al., 2010)	40
Table 2.4	List of different additive that add to the ZTA	45
Table 3.1	Raw materials are used in this study	56
Table 3.2	Amount of raw material that mixed for ZTA-SrCO ₃	60
Table 3.3	Amount of raw material that mixed for ZTA-MgO samples	60
Table 4.1	XRD quantitative analysis of the samples with different amount of SrCO ₃	100
Table 4.2	Correlation coefficient (R), mean absolute relative error (MARE) for different methods	130

LIST OF FIGURES

		Page
Figure 1-1	North American technical and advanced structural ceramics marketed based on applications (Wellesley, 2012)	2
Figure 1-2	Penetration process in ceramic armor (Shockey et al., 1990)	4
Figure 1-3	Overview of research	8
Figure 2-1	Penetration in the ceramic armor (a) dwell, (b) crashed cone in ceramic is formed, (c) deformed the back plate, and(d) backing plate failed	13
Figure 2-2	Schematic of fix target test (Normandia & Gooch, 2002)	16
Figure 2-3	Different configuration of depth of penetration (James, 2002)	17
Figure 2 4	Apparatus developed by Bertram Hopkinson for the measurement of pressure produced by the detonation of gun cotton(Gama et al., 2004)	19
Figure 2-5	Schematic of Kolsky's apparatus(Gama et al., 2004)	19
Figure 2-6	Schematic illustration of material response and incident pulse of SHPB (a) Rectangular shaped pulse for ductile materials, (b) Rectangular shaped pulse for brittle materials, and (c) Ramp shaped pulse for brittle materials (Subhash & Ravichandran, 2000)	25

Figure 2-7	Schematic of hydraulic confinement(Chen & Lu, 2000)	27
Figure 2-8	The schematic illustration of the confining the sample with thin sleeve (Chen & Ravichandran, 1996)	28
Figure 2-9	Applying 3 axial load in testing the specimen with SHPB	29
Figure 2-10	Schematic overview of how crack start in ceramic (a) grain boundary debonds and voids, (b) foreign particles such as inclusions, (c)dislocation pileups, (d)twins and staking faults, and (e)dilatant crack produced by elastic anisotropy (Shih et al., 2000)	30
Figure 2-11	Schematic of wing crack is started from tip of flaws (Ravichandran & Subhash, 1995)	33
Figure 2-12	Fracture in the ceramic by dynamic uniaxial load (Chen et al., 2007)	35
Figure 2-13	Fracture in the specimen with surface defeat under uniaxial dynamic load (Chen et al., 2007)	35
Figure 2-14	Fracture in the specimen under multi axial dynamic load (Chen et al., 2007)	36
Figure 2-15	(a)Intact ZTA armor vest, and (b) Damage ZTA armor vest (Wells et al., 2009)	37
Figure 2-16	The projectile performed in the ZTA armor (Nayak et al.,2013)	38
Figure 2-17	The structure and interface of anti-sandwich structure (Zhou et al., 2014)	38

Figure 2-18	Micrograph for (a)pure alumina, (b)10% ZTA, (c)20%ZTA, (d)30%ZTA, (e)40%ZTA, and (f)pure zirconia (Oungkulsolmongkol et al., 2010)	40
Figure 2-19	Phase diagram of alumina and zirconia (Lakiza & Lopato, 1997)	41
Figure 2-20	Phase diagram of Alumina SrO (Vishista & Gnanam, 2006)	47
Figure 2-21	Hardness and fracture toughness of ZTA with Cr ₂ O ₃ (Azhar et al., 2012)	48
Figure 2-22	The similarity of the cell and artificial neural network (Ghaboussi et al., 1991)	50
Figure 2-23	Schematic structure of neural network for strain rate depend material	53
Figure 3-1	Flowchart of the thesis	55
Figure 3-2	Molds used for preparation of the samples a) mold diameter is 6mm (used for preparing sample for SHPB), and b) mold diameter is 12 mm	57
Figure 3-3	Sintering profile of samples	58
Figure 3-4	Sample preparation flowchart	59

Figure 3-5	Crack due to the Vickers hardness indentation test a) schematic and b) FESEM image of Vickers hardness test and cracks	63
Figure 3-6	Schematic set up of the SHPB apparatus	64
Figure 3-7	SHPB and high speed camera setup	64
Figure 3-8	Generated pulse shapes (a) without WC, and (b) with WC	66
Figure 3-9	Sample sandwiched between two WC platens	67
Figure 3-10	Pulse changing (a) pulse before attached with the copper pulse shaper, and (b) pulse after attached with the copper pulse shaper	68
Figure 3-11	Copper pulse shaper	69
Figure 3-13	Incident, reflected and transmitted wave responses captured from the SHPB apparatus	70
Figure 3-12	SHPB operation menu	70
Figure 3-14	Installing the sleeve for ceramic sample	72
Figure 3-15	SHPB transmission wave for copper sleeve	73
Figure 3-16	SHPB transmission wave for brass sleeve	73
Figure 3-17	The structural of the MLP neural network	75
Figure 3-18	Schematic design of time series algorithm (a) Open loop, and (b) Close loop	77
Figure 3-19	Schematic view of time series neural network	78

Figure 3-20	Nonlinear regression with ϵ insensitive band in the SVR	80
Figure 4-1	Result of particles size analysis for Al_2O_3 particles.	82
Figure 4-2	Morphology of Al_2O_3 particles at 5K magnification.	82
Figure 4-3	XRD result for Al_2O_3 powders, ICDD reference 00-10-0173.	83
Figure 4-4	Results of particle size for YSZ particles.	83
Figure 4-5	Morphology of YSZ particles at 5K magnification.	84
Figure 4-6	XRD results for YSZ powders, ICDD reference file for tetragonal (t) and monoclinic (m) are 00-89-9068 and 00-78-1808 respectively.	85
Figure 4-7	Particle size analysis of the SrCO_3	85
Figure 4-8	XRD result of the SrCO_3	86
Figure 4-9	Morphology of SrCO_3	86
Figure 4-10	Particle size analysis of the MgO	87
Figure 4-11	MgO XRD result	87
Figure 4-12	Morphology of MgO	88
Figure 4-13	Effect of YSZ addition in ZTA on fracture toughness and hardness	89
Figure 4-14	XRD result of different composition of ZTA	89
Figure 4-15	Effect of YSZ on density and porosity of sample	90

Figure 4-16	Microstructure of (a) pure alumina, (b)10 wt.% YSZ, (c) 20 wt.% YSZ, (d) 30 wt.% YSZ, and (e) 40 wt.% YSZ	91
Figure 4-17	Crack propagation for (a) 10 wt.% YSZ, (b) 20 wt.% YSZ, (c) 30 wt.% YSZ, and (d) 40 wt.% YSZ	93
Figure 4-18	Stress and strain of ZTA with different YSZ percentage	94
Figure 4-19	Maximum dynamic stress vs of YSZ (wt%)	94
Figure 4-20	(a) Schematic distribution of flaws and developing the wing crack under the compressive loading, (b) crack growth under the compressive load, (C) Effect of the neighboring crack in the crack propagation	97
Figure 4-21	XRD result of different composition of ZTA-SrCO ₃	99
Figure 4-22	Microstructure of ZTA samples added with various amount of SrCO ₃ . (a)1wt.% SrCO ₃ , (b) 2 wt.% SrCO ₃ , (c) 3 wt.% SrCO ₃ , (d) 4 wt.% SrCO ₃ (e) 5 wt.% SrCO ₃ and (g) enlargement of SrAl ₁₂ O ₁₉ grain shape	100
Figure 4-23	Bulk density and percentage of porosity for ZTA samples as a function of SrCO ₃	101
Figure 4-24	The hardness and fracture toughness of ZTA-SrO as function of SrCO ₃	102
Figure 4-25	Fracture mechanism in the ZTA with different percentage of SrCO ₃ , (a)1% SrCO ₃ , (b) 2% SrCO ₃ , (c) 3% SrCO ₃ , (d) 4% SrCO ₃ , and (e) 5% SrCO ₃	103

Figure 4-26	Dynamic Stress and strain curve of ZTA with different percentage of SrCO ₃	106
Figure 4-27	Maximum dynamic compressive stress of different composition of ZTA-SrCO ₃	107
Figure 4-28	Failure of the ZTA-2% SrCO ₃ during the SHPB test (a) Intact sample, (b) crack started from the contact surfaces of the bars and sample, (c) crack propagation and more fragment, and (d) sample failure	109
Figure 4-29	Effect of MgO addition in ZTA on fracture toughness and hardness	110
Figure 4-30	XRD result of different composition of ZTA-MgO	112
Figure 4-31	Effect of MgO on density and porosity of sample	113
Figure 4-32	Microstructure of (a) 0.2 wt.%MgO, (b) 0.5 wt.%MgO, (c) 0.7 wt.%MgO, and (d) 0.9 wt.%MgO	114
Figure 4-33	Crack propagation for (a) 0.2wt.% MgO, (b) 0.5 wt.% MgO, (c) 0.7 wt.% MgO, and (d) 0.9 wt.% MgO	115
Figure 4-34	Dynamic Stress and strain curve of ZTA with different percentage of MgO	117
Figure 4-35	Maximum dynamic compressive stress of ZTA added with different amount of MgO	118
Figure 4-36	The Relationship between the hardness and dynamic strength	120

Figure 4-36	The Relationship between the hardness and dynamic strength	120
Figure 4-37	Relationship between the dynamic strength, hardness and fracture toughness	121
Figure 4-38	Stress-Strain curve of the sample under different confinement and strain-rate	122
Figure 4-39	Crack propagation in sample by confinement under the dynamic load	123
Figure 4-40	Regression between the output of MLP network (8-8 architecture) and target	124
Figure 4-41	Compering the prediction of MLP and SVR with experimental data	126
Figure 4-42	Prediction of time series neural network	128
Figure 4-43	Error of prediction for all machine learning methods	129

LIST OF ABBREVIATIONS

ZTA	-	Zirconia toughend Alumina
YSZ	-	Yttria stablized Zirconia
SHPB	-	Split Hopkinson Pressure Bar
EDX	-	Energy Dispersive X-ray
FESEM	-	Field Emission Scanning Microscope Electron
SEM	-	Scanning Microscope Electron
XRD	-	X- ray diffraction
Wt%	-	Weight percentage
ICDD	-	International Center For Diffraction

LIST OF SYMBOLS

A_b	cross sectional area of the bar
E_b	Young's modulus of the bar
C_b	longitudinal elastic wave speed
P	Pressure
V	Velocity
σ	Stress
ε	Strain
$\dot{\varepsilon}$	Strain Rate
A_s	Cross-sectional area of the sample
L_s	Length of the sample
δ	Misfit
r	Radius
ν	Poisson's ratio
σ_y	Yield strength
t	Thickness of the sleeve
D	Outer diameter of the sleeve
H	Vickers hardness
k_{IC}	Fracture toughness
l_e	Effective crack length
P_r	Porosity
e^n	Total error for n -th iteration
d_j^n	Target output
y_j^n	Network output

EKSPERIMENTAL PENCIRIAN DAN RAMALAN RANGKAIAN NEURAL UNTUK SIFAT DINAMIK ZTA DENGAN SrCO₃ DAN MgO

ABSTRAK

Bahan seramik digunakan dengan meluas dalam alatan ketenteraan kerana sifat-sifat bahan yang menarik seperti kekerasan yang tinggi dengan ketumpatan yang rendah dan kekuatan mampatan yang tinggi. Walau bagaimanapun, untuk mereka bentuk dan pemilihan bahan seramik yang sesuai memerlukan pengetahuan yang mendalam mengenai perlakuan dinamik seramik. Beberapa kajian telah dilakukan ke atas perlakuan dinamik seramik, namun begitu kebanyakan kajian yang dilakukan hanya terhad ke atas seramik konvensional seperti Al₂O₃, B₄C, SiC. Atas sebab ini, ramalan ke atas perlakuan dinamik bagi komposisi seramik baru adalah sukar dan untuk beberapa ketika ia adalah mustahil. Dalam kajian ini, sifat-sifat mekanikal dan perlakuan dinamik ZTA dikaji. Kajian perlakuan dinamik ZTA menggunakan alatan SHPB yang di ubah suai (memasang 'pulse shaper' dan bahan di letakkan antara plate we. Kesan penambahan YSZ (10-40 wt.%) ke atas sifat-sifat bahan ZTA turut dikaji secara dinamik menggunakan SHPB. Penambahan 20 wt.% YSZ ke dalam ZTA menunjukkan sifat-sifat bahan dan perlakuan dinamik yang optimum. Kesan penambahan SrCO₃ (1-5wt.%) ke dalam ZTA dengan 20 wt.% YSZ dan pembentukan fasa (SrAl₁₂O₁₉) mempengaruhi keliangan dan keliatan retak. Pembentukan fasa ini meningkatkan keliangan dan justeru merendahkan prestasi dinamik komposit tersebut. Penambahan MgO (0.2-0.9 wt.%) ke dalam ZTA dengan 20 wt.% YSZ menyebabkan pengecilan saiz butir dan mengakibatkan peningkatan kekerasan. Kajian juga dilakukan bagi keadaan bebanan dinamik yang berbeza ke atas ZTA dengan 20 wt.% YSZ dan 0.2 wt.% MgO. Perlakuan dinamik ZTA diramal menggunakan 3 kaedah mesin pembelajaran yang berbeza iaitu 'Multilayer Perceptron (MLP)', 'Time Series'

dan 'Supporting Vector Regression (SVR)'. Setiap kaedah ramalan dibandingkan, dan kaedah 'Time Series' melalui rangkaian neural menunjukkan keputusan terbaik yang sama dengan data eksperimen.

EXPERIMENTAL CHARACTERIZATION AND NEURAL NETWORK PREDICTION OF DYNAMIC BEHAVIOR OF ZTA WITH SrCO₃ AND MgO

ABSTRACT

Ceramics materials are extensively used in armor applications for their attractive properties such as high hardness, low density and high compressive strength. However for designing and selection for appropriate ceramic armor material, a deep knowledge about the dynamic behavior of ceramic is necessary. A number of research has been done on dynamic behavior of ceramic, unfortunately most of work focused on the conventional and limited ceramics (such as Al₂O₃ , B₄C, SiC). For this reason prediction of the dynamic behavior of the new composition of ceramics is difficult and some time is impossible. In this work, mechanical properties and dynamic behavior of ZTA are being investigated. For studying the dynamic behavior of the ZTA, SHPB apparatus is modified (using pulse shaper and sandwich the sample with WC platen) and used. Effect of different amount of YSZ (10-40wt.%) on their properties of ZTA is also investigated dynamically using SHPB. ZTA with 20 wt.% YSZ shows the optimum properties and also their dynamic behavior. Effect of SrCO₃ (1-5wt.%) added to the ZTA with 20 wt.% YSZ and the formation of new phase (SrAl₁₂O₁₉) on porosity and fracture toughness is of interest. The formation of this phase increases the porosity and hence decreases the dynamic performance of the composite. An addition of MgO (0.2-0.9wt.%) to ZTA with 20 wt.% YSZ resulted a reduction in grain size and consequently increase the hardness. Further investigation on different dynamic loading condition on ZTA with 20 wt.% YSZ and 0.2wt.% MgO were also conducted. The dynamic behavior of representative ZTA is predicted by three different machine learning methods (Multilayer Perceptron (MLP), Time Series and Supporting Vector

Regression (SVR)). The predictions are compared to each other and the time series neural networks shows the best agreement with the experimental data.

CHAPTER 1

INTRODUCTION

1.1 Research background

Ceramics materials can be defined as “Any inorganic and non-metallic product prepared by treatment at temperatures higher than 540°C (1,000°F) or used under conditions implying these temperatures, which includes metallic oxides and borides, carbides, nitrides and mixtures of these compounds” (Boch & Niepce, 2010). Ceramic materials have interesting properties, including refractoriness, high melting point, high strength at high temperature, and applicable mechanical properties (compressive strength, hardness, erosion resistance, wear resistance). In the light of these attractive combination of properties, ceramics material has high potential to be candidate in many different application. However these comprehensive application are limited because of the brittleness and variability in mechanical properties.

Ceramic materials are mainly used in six main applications i.e. bioceramic, armor and military, wear and erosion, cutting tools, energy and high temperature and aircraft and aerospace equipment (Rosso, 2006). Figure 1-1 shows the value of these application in the North America market. Bioceramic become the biggest segment of the ceramic applications followed by armor and military application (Wellesley, 2012).

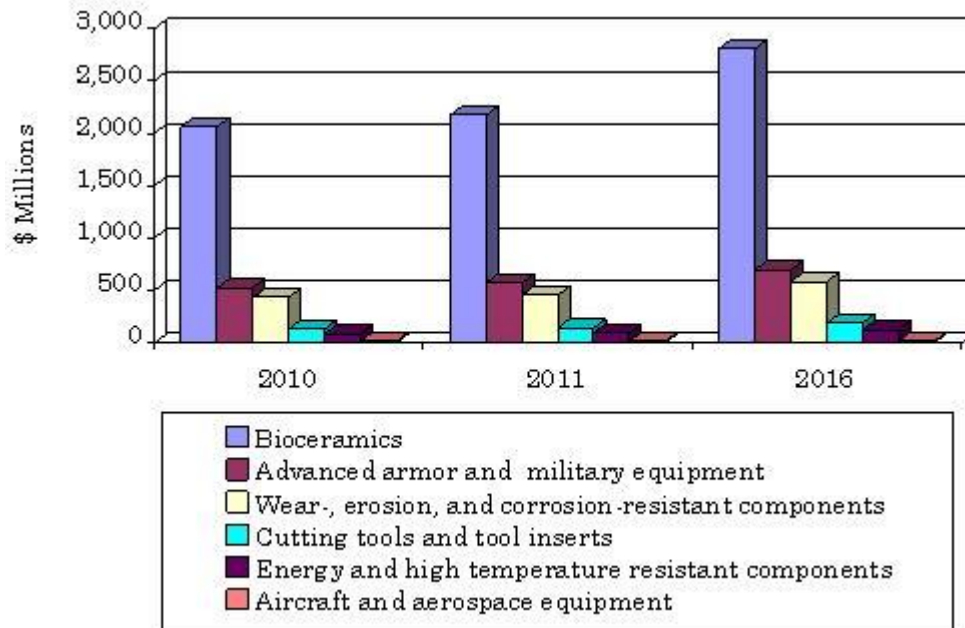


Figure 1-1 North American technical and advanced structural ceramics marketed based on applications (Wellesley, 2012)

History shows that the armors developed in parallel with the development of weapons. There are many different materials used for the armor application. One of the first recorded example of the use of body armors was by the medieval Japanese who used armor manufactured from silk to withstand from arrow penetration (Turnbull, 2012). Later with the progress in the weaponry technology, metals were used as an armor. But modern projectiles are able to penetrate the metal armors, thus the armor designer are looking for new materials that can stand against modern projectiles. Ceramic is a good candidate for armor. The ceramic usage as armor has started after WWII. This application was extended when the ceramic armor save the life of the many helicopter's pilot during the Vietnam War (Walley, 2010).

Ceramics offer many attractive properties for armor application, such as high specific stiffness, high specific strength, low thermal conductivity, and chemical inertness in various environments. The unique combination of low density (lightweight), superior hardness and high compressive strength compared to metals